ELSEVIER

Journal of Power Sources 86 (2000) 173–180

JOURNAL OF POWER SOURCES

www.elsevier.com/locate/jpowsour

Development and application of a generalised steady-state electrochemical model for a PEM fuel cell

Ronald F. Mann *, John C. Amphlett, Michael A.I. Hooper, Heidi M. Jensen, Brant A. Peppley, Pierre R. Roberge

Electrochemical Power Sources Group, Department of Chemistry and Chemical Engineering, Royal Military College of Canada, Kingston, Ontario, Canada K7K 7B4

Accepted 12 November 1999

Abstract

Models have previously been developed and published to predict the steady-state performance of solid polymer electrolyte membrane fuel cells (PEMFC). In general, such models have been formulated for particular fuel cells and have not been easily applicable to cells with different characteristics, dimensions, etc. The development of a generic model is described here that will accept as input not only values of the operating variables such as anode and cathode feed gas, pressure and compositions, cell temperature and current density, but also cell parameters including active area and membrane thickness. A further feature of the model is the addition of a term to account for membrane ageing. This term is based on the idea that the water-carrying capacity of the membrane deteriorates with time in service. The resulting model is largely mechanistic, with most terms being derived from theory or including coefficients that have a theoretical basis. The major nonmechanistic term is the ohmic overvoltage that is primarily empirically based. The model is applied to several sets of published data for various cells which used platinum as the anode catalyst. Data for various PEM cell designs were well correlated by the model. The lack of agreement of the model predictions with some experimental results may be due to differences in the characteristics of the electrocatalyst. The value of such a generic model to predict or correlate PEM fuel cell voltages is discussed.

Keywords: PEM fuel cell; Electrochemical model

1. Introduction

Many mechanistic models [1–6] and empirical models [8–12] can be found in the literature. While the level of complexity associated with these models varies considerably, one can clearly trace the evolution of the electrochemical model for polymer electrolyte membrane fuel cells over the last decade. The recent work of Lee et al. [12] displays the most comprehensive form of empirical model produced to date to predict the current/voltage relationship for the typical PEMFC.

$$V = V_0 - b \ln i - Ri - m \exp(ni) - b \ln\left(\frac{P}{P_{O_2}}\right) \qquad (1)$$

where b, R, m and n are all empirical parameters that are functions of the operating conditions.

Lee's model features the familiar terms representing activation polarisation and Ohm's Law contributions, as well as incorporating two terms which have appeared only recently in the literature — an exponential term and a *pressure ratio logarithm* that serve to model the effects of concentration polarisation predominantly at higher current densities. The logarithmic term was first presented by Kim et al. [11] without a physicochemical interpretation, although more recent works have offered some limited insight into the nature of the exponential coefficient, n [13]. The pressure ratio logarithm term appears to be a new attempt to fit experimental data. The model itself highlights the pitfalls of empirical modelling — the exponential term has no physical justification and serves merely as a curve-fitting tool; consequently, it is of extremely limited use as a predictive instrument until such time as the nature of the coefficients, n and m, are understood; presently, the coefficients must be re-evaluated for any change in operating conditions. The model also elucidates the major diffi-

* Corresponding author.

0378-7753/00/$ - see front matter
PII: S0378-7753(99)00484-X

culty associated with mechanistic modelling, namely the complex nature of the relationships between key variables governing the various sources of overpotential within the PEMFC. Lee's model presents all variables as functions of temperature, pressure, oxygen concentration and humidity, all of which, in the strictest sense, vary locally in at least two dimensions. Lee does assume local variation of these values although there is no mention made of other established relationships which would certainly be present in a mechanistically based model, such as that shared by humidity and membrane local water content [14], inter alia.

At the opposite end of the PEMFC model spectrum, Eikerling et al. [5] have recently presented a mechanistic model that is impressive in its consideration of variable interrelations. The model treats all variables with a local description, thereby allowing for consideration of membrane water content gradients and local, rather than global, dehydration effects. The Eikerling paper provides considerable insight into the nature and role of water transport in the polymeric membrane; the convective model presented therein can be seen to elucidate trends in experimental data. The complexity of the model is intimidating, however, presenting membrane conductivity as a function of the Heaviside Step Function and membrane water content; the latter is, in turn, dependent upon anode and cathode gas pressures, local liquid water pressure and membrane thickness. Analytical expressions are presented for several different operating conditions, including operation near the limiting current density as well as under an anode/cathode gas pressure differential, with assumptions of diffusion and convection-controlled transport. Given the complexity of the resultant model, and bearing in mind that it is still one-dimensional and isothermal, one quickly generates a respect for the rather intricate nature of the processes that must be modelled to accurately predict fuel cell performance.

Springer, Gottesfeld and Zawodzinski [4,15,16] have also achieved considerable success in PEMFC modelling over the last decade. Rather than appearing to converge towards a generally accepted model, their cumulative efforts have generated increasingly complex predictors of cell performance as the interdependencies of variables and the nature of transport processes and other fuel cell phenomena are better understood. The *along-the-channel model* of Yi and Nguyen [7] highlights the added considerations associated with incorporation of temperature and pressure gradients across the membrane. A more recent article by the same authors [17] displays the changes to the associated model which must be effected when design changes shift the governing form of gaseous transport within the cell, that is, from diffusion to forced convection.

This laboratory [18–22] has previously proposed a steady-state electrochemical model (SSEM) for PEM fuel cells and has applied it to particular cells manufactured by Ballard Power Systems of Burnaby, BC, Canada. This SSEM had both mechanistic and empirical features but was still restricted in its application to two particular cells: the Ballard Mark IV and Mark V vintage 1988 to 1990.

The goals of the present work were:

(a) to modify and generalise the terms in the SSEM which were specific to the Ballard cells,

(b) to introduce cell dimensions and characteristics as input parameters,

(c) to extend the useful range of the SSEM to higher current densities above about 0.5 A/cm^2.

The result of this work has been called the generalised steady-state electrochemical model (GSSEM) to distinguish it from the previous SSEM.

2. Model development

2.1. General

PEM fuel cells consist of three major components — an anode, typically featuring a platinum or platinum-containing catalyst, a thin, solid polymeric sheet which acts as electrolyte, and a cathode, also platinum-catalysed. The various reactions for a PEM fuel cell fed with a hydrogen-containing anode gas and an oxygen-containing cathode gas, are:

Anode: $H_2 \rightleftarrows 2H^+ + 2e^-$

Cathode: $2H^+ + 2e^- + 1/2O_2 \rightleftarrows H_2O$

Overall: $H_2 + 1/2O_2 \rightleftarrows H_2O$

The products of this process are dc electricity, liquid water and heat.

The basic expression for the voltage for a single cell is:

$$V_{\text{Cell}} = E_{\text{Nernst}} + \eta_{\text{act, a}} + \eta_{\text{act, c}} + \eta_{\text{ohmic}} \quad (2)$$

where: E_{Nernst} is the thermodynamic potential, $\eta_{\text{act, a}}$ is the anode activation overvoltage, a measure of the voltage loss associated with the anode, $\eta_{\text{act, c}}$ is the cathode activation overvoltage, a measure of the voltage loss associated with the cathode, and η_{ohmic} is the ohmic overvoltage, a measure of the IR losses associated with the proton conductivity of the solid polymer electrolyte and electronic internal resistances. All quantities in Eq. (2) are in units of volts.

The three overvoltage terms are all negative in the above expression and represent reductions from E_{Nernst} to give the useful cell voltage, V_{Cell}. Each of the terms in Eq. (2) will now be separately discussed and modelled.

2.2. Thermodynamic potential, E_{Nernst}

As developed earlier [18,19], the Nernst equation for the hydrogen/oxygen fuel cell, using literature values for the standard-state entropy change, can be written:

$$E_{\text{Nernst}} = 1.229 - (8.5 \times 10^{-4})(T - 298.15) + (4.308 \times 10^{-5})T(\ln p^*_{H_2} + 1/2 \ln p^*_{O_2}) \quad (3)$$

where T is the cell temperature (K), $p^*_{H_2}$ is the partial pressure of hydrogen at the anode catalyst/gas interface (atm), and $p^*_{O_2}$ is the partial pressure of oxygen at the cathode catalyst/gas interface (atm).

Evaluation of the two partial pressures typically involves mass transfer calculations and normally requires averaging over a cell surface or along the direction of gas flow, to account for significant changes in the bulk phase partial pressures of the gaseous reactants due to reaction in the cell. This has been fully discussed previously [20].

2.2.1. The anode overvoltage

As proposed by Berger [23] and described earlier [20], the anode overvoltage can be represented by:

$$\eta_{act,a} = -\frac{\Delta G_{ec}}{2\mathcal{F}} + \frac{RT}{2\mathcal{F}}\ln\left(4\mathcal{F}Ak^0_a c^*_{H_2}\right) - \frac{RT}{2\mathcal{F}}\ln i \qquad (4)$$

where ΔG_{ec} is the standard-state free energy of activation for chemisorption (J/mol), $\mathcal{F}$ is Faraday's constant (96,487 C/equ.), A is the active cell area (cm^2), k^0_a is the intrinsic rate constant (cm/s) for the anode reaction, $c^*_{H_2}$ is the liquid-phase concentration of hydrogen at the anode membrane/gas interface (mol/cm^3), i is the current (amps), and R is the gas constant (J/mol K).

Eq. (4), after the insertion of the known parameter values and rearrangement, gives:

$$\eta_{act,a} = -(5.18\times10^{-6})\Delta G_{ec} + (4.309\times10^{-5}) \times T\left[12.863 + \ln\left(\frac{Ac^*_{H_2}\cdot k^0_a}{i}\right)\right] \qquad (5)$$

In Eq. (5), ΔG_{ec} and k^0_a are chemical parameters of the reaction, initially unknown, while T, A, $c^*_{H_2}$ and i can all be quantified for a particular simulation calculation.

2.3. The cathode overvoltage

Again, as previously proposed [23] and described [20], the cathode overvoltage can be given by

$$\eta_{act,c} = \frac{RT}{\alpha_c\mathcal{F}n}\left(\ln\left[n\mathcal{F}Ak^0_c\exp\left(-\frac{\Delta G_e}{RT}\right) \times (c^*_{O_2})^{(1-\alpha_c)}(c^*_{H^+})^{(1-\alpha_c)}(c^*_{H_2O})^{\alpha_c}\right] - \ln i\right) \qquad (6)$$

According to Berger [24], the rate-controlling step for the reduction of oxygen is likely to be:

$$M(OH) + H^+ \rightleftarrows H_2O$$

where ''M'' represents an active site on the platinum cathode catalyst. The value of n for this step is unity and this value will, therefore, be used in Eq. (6).

As previously argued [10], both $c^*_{H^+}$ and $c^*_{H_2O}$ in Eq. (6) should be relatively constant at the membrane/gas interface on the cathode side of the cell. Incorporating these into k^0_c (to give k'_c) and inserting all the known parameter values produces:

$$\eta_{act,c} = \frac{1}{\alpha_c}\left[-(10.36\times10^{-6})\Delta G_e + (8.62\times10^{-5}) \times T\left(12.863 + \ln A + \ln k'_c + (1-\alpha_c)\ln c^*_{O_2} - \ln i\right)\right] \qquad (7)$$

where $k'_c = k^0_c c^*_{H^+} c^*_{H_2O}$

Similar to Eq. (5), ΔG_e, α_c and k'_c in Eq. (7) are chemical parameters of the cathode reaction while T, A, $c^*_{O_2}$, and i can all be quantified for a particular simulation calculation.

2.4. Total activation overvoltage

If there is a need for a single expression to represent the activation overvoltage, Eqs. (4) and (6) can be summed to give, as previously published [20]:

$$\eta_{act} = \xi_1 + \xi_2 T + \xi_3 T\left[\ln(c^*_{O_2})\right] + \xi_4 T\left[\ln(i)\right] \qquad (8)$$

where:

$$\xi_1 = -\frac{\Delta G_{ec}}{2\mathcal{F}} - \frac{\Delta G_e}{\alpha_c n\mathcal{F}} \qquad (8a)$$

$$\xi_2 = \frac{R}{\alpha_c n\mathcal{F}}\ln\left[n\mathcal{F}Ak^0_c(c^*_{H^+})^{(1-\alpha_c)}(c^*_{H_2O})^{\alpha_c}\right] + \frac{R}{2\mathcal{F}}\ln\left[4\mathcal{F}Ak^0_a c^*_{H_2}\right] \qquad (8b)$$

$$\xi_3 = \frac{R(1-\alpha_c)}{\alpha_c n\mathcal{F}} \qquad (8c)$$

$$\xi_4 = -\left(\frac{R}{2\mathcal{F}} + \frac{R}{\alpha_c n\mathcal{F}}\right) \qquad (8d)$$

2.5. The ohmic overvoltage

Ohmic polarisation should result from resistance to electron transfer in the graphite collector plates and graphite electrodes plus resistance to proton transfer in the solid polymer membrane. This could be expressed using Ohm's Law equations such as:

$$\eta_{ohmic} = \eta^{electronic}_{ohmic} + \eta^{proton}_{ohmic} = -i(R^{electronic} + R^{proton}) = -iR^{internal} \qquad (9)$$

Experimental measurement of $R^{internal}$ might also involve additional contact resistances that are lumped into $R^{electronic}$.

Resistance to electron flow should be approximately constant over the relatively narrow temperature range of PEM fuel cell operation, perhaps 50°C to 90°C at most. The parameter $R^{\text{electronic}}$ could, therefore, be taken as a constant, but is generally difficult to predict and, therefore, is initially an unknown.

Resistance to proton flow, as described earlier [20], will be a complicated function of water content and distribution in the membrane, both of which will be further dependent on operating parameters such as T and i. Although water distribution in PEM membranes has been extensively studied [4–6,24–29], an empirical approach to the prediction of R^{proton} has been adopted here. The recommendations of Springer et al. [4] and the data of Buchi and Scherer [33] were used to formulate the empirical relationship formula for R^{proton}, although the theoretical development of Eikerling et al. [5] also provided insight to the process.

A general expression for resistance was defined to include all the important membrane parameters:

$$R^{\text{proton}} = \frac{r_{\text{M}} l}{A} \tag{10}$$

where r_{M} is the membrane specific resistivity for the flow of hydrated protons (ohm.cm), and l is the thickness of the polymer membrane (cm), which serves as the cell electrolyte.

In Eq. (10), A and l are known dimensional parameters for a particular cell while r_{M} will be a function of the type and characteristics of the membrane, temperature, water content or degree of hydration of the membrane, and current density. The major problem at this point is the development of an empirical expression for r_{M} that takes all of these independent variables into account. Nafion membrane, a trademark preparation of Dupont, is widely used in PEM fuel cells and will be the only membrane considered in this paper — partly due to its wide use and partly due to the large amount of published resistivity or conductivity data [4]. It should be noted that there is some confusion in the literature over Nafion nomenclature and characteristics. Dupont uses the following product designations to denote Nafion membrane thickness:

Nafion 117: 7 mil (178 μm)
Nafion 115: 5 mil (127 μm)
Nafion 112: 2 mil (51 μm)

while Springer et al. [4] refer to Nafion 117 with thicknesses of 50, 100, 140 and 175 μm. Springer's results will be interpreted as all being for Nafion membranes but only the 175-μm data being for Nafion 117. Prater [31] reports Nafion 117 membrane thicknesses from 210 to 222 μm while Buchi and Scherer [33] report 203 μm. In all cases, Nafion with an equivalent weight of 1100 is being utilized.

Based on the recommendations of Springer et al. [4], the data of Buchi and Scherer [33] and on the correlation of the sets of published PEM fuel cell performance curves reported in Figs. 1–5, the following empirical expression for Nafion membrane resistivity is proposed:

$$r_{\text{M}} = \frac{181.6\left[1 + 0.03\left(\frac{i}{A}\right) + 0.062\left(\frac{T}{303}\right)^2\left(\frac{i}{A}\right)^{2.5}\right]}{\left[\lambda - 0.634 - 3\left(\frac{i}{A}\right)\right]\exp\left(4.18\left[\frac{T-303}{T}\right]\right)} \tag{11}$$

where: $181.6/(\lambda - 0.634)$ is the specific resistivity (ohm.cm) at zero current and 30°C and the exponential term in the denominator is the temperature correction factor if the cell is not at 30°C where T is the cell absolute temperature in Kelvin degrees, both derived from Springer et al. [4]. The term in square brackets in the numerator was derived from a fit of the resistance data in Fig. 6 of Buchi and Scherer [33] and, in conjunction with the $3(i/A)$ reduction in the λ term, represent an empirical correction to the specific resistivity to bring in two other factors that affect the average water content of the membrane-current density and cell temperature. The parameter, λ, described in Fig. 2 and Eq. 16 of Springer et al. [4], can have a value as high as 14 under ideal, 100% relative humidity conditions and has had reported values as high as 22 [4] and 23 [33] under supersaturated conditions. In this work, λ is being considered as an adjustable parameter with a possible maximum value of 23 and is, therefore, the major fitting parameter in Figs. 1–5. The parameter λ will be influenced by the membrane preparation procedure, will be a function of the relative humidity and stoichiometric ratio of the anode feed gas, and will likely also be a function of the age (time-in-service) of the membrane.

2.6. Summary of model

Thus, the preliminary GSSEM can be seen to consist of Eqs. (2), (3), (5), (7)–(11). These equations, combined in an appropriate algorithm that supplies the appropriate val-

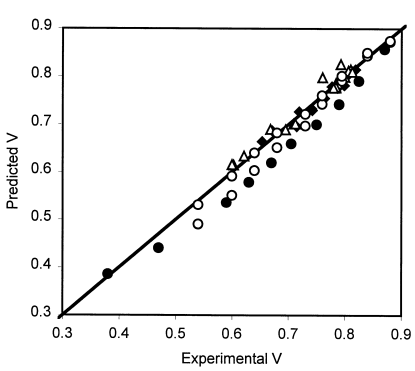

Fig. 1. H_2/air multicase comparison optimal coefficients: $\lambda = 14.0$. Prater [31] (●), Amphlett et al. [19], Table 2 (△), Amphlett et al. [19], Table 3 (♦), Watkins et al. [30] (○).

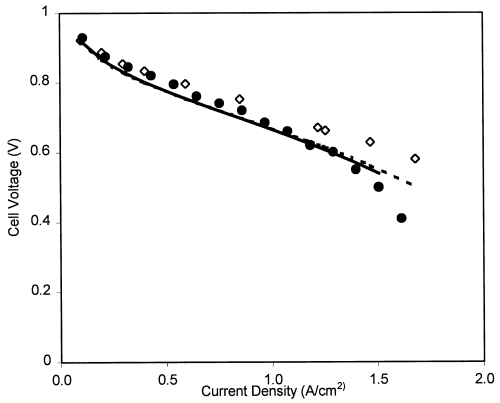

Fig. 2. Performance curve comparison for H_2/O_2 cells: $\lambda = 23.0$, Prater [31] (70°C) (●), Watkins et al. [30] (◇). GSSEM prediction for Prater conditions (————), GSSEM Prediction for Watkins et al. conditions (---).

ues of the operating conditions at the catalyst/membrane interface, are able to predict the voltage output of PEM fuel cells of various configurations.

3. Further quantitative development of the activation overvoltage expression

3.1. Overview

The proposed single expression for the total activation overvoltage, Eq. (8), can be further developed using results from previous experimental studies of Ballard Power Systems hardware carried out in these laboratories.

3.1.1. Ballard Power Systems Mark IV PEMFC

Data from the Mark IV fuel cell, a late-1980's technology, have been extensively published but the present analysis will concentrate on results from this laboratory [18,20,21] for which all operating conditions are clearly known. The hardware under study was a single cell with

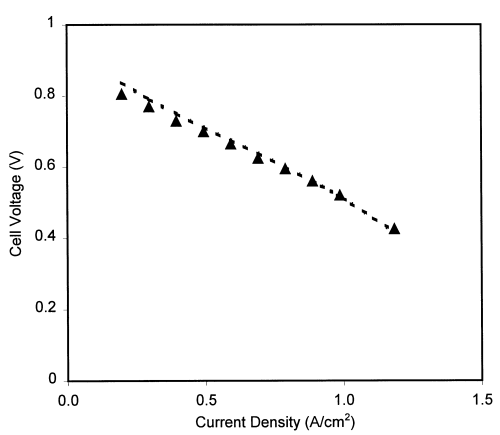

Fig. 3. Performance curve of H_2/O_2 cells. Kim et al. [11]. Nafion 115 membrane, and 70°C. $\lambda = 12.5$.

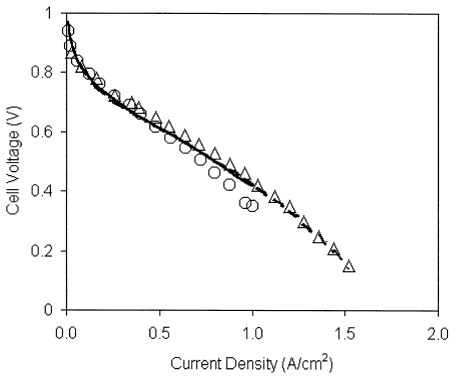

Fig. 4. H_2/O_2 data of Paganin et al. [32]. Nafion 117 membrane, 80°C (△) and 70°C (○). Prediction of GSSEM, 80°C (– – –), prediction of GSSEM, 70°C (————).

an active cell area of 50.6 cm^2, although some data from a 12-cell stack were also included in the evaluation.

The single cells had experienced approximately 500 h of noncontinuous operation at the start of the approximately 75-h experimental program; they had already shown a significant drop in cell voltage from their new condition, approx. 0.1 V at 0.44 A/cm^2, 70°C, 30 psig air and H_2. No further voltage degradation was observed during the experimental program.

Referring to Eq. (8), experimental values have been published [21] for the various coefficients:

$$\xi_1 = -0.9514 \quad \xi_2 = 0.00312$$

$$\xi_3 = 7.4 \times 10^{-5} \quad \xi_4 = -0.000187$$

Utilising the above coefficients in the various terms of Eq. (8) gives:

(i) $\alpha_c = 0.60$ from ξ_4
(ii) $\alpha_c = 0.54$ from ξ_3
(iii) $\Delta G_{ec} + 3.51(\Delta G_e) = 1.836 \times 10^5$ J/mol
(iv) $k_c^0 (c^*_{H^+})^{(1-\alpha_c)} (c^*_{H_2O})^{\alpha_c} (k_c^0)^{0.285} \cong 61.7$ to 76.5

The above range of numerical values for (iv) is, at least partially, due to one of the assumptions originally made by Baumert [18] and used later [19–21] that is not quite true. The case was made [20] that $c^*_{H_2}$ in Eqs. (4) and (5) would not vary significantly over the various trials in the test

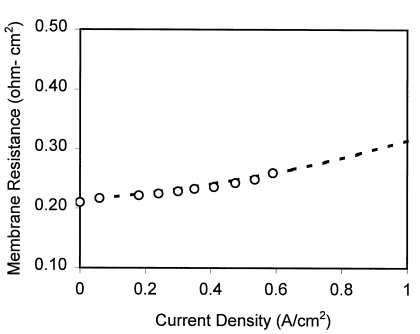

Fig. 5. Prediction of membrane resistance of GSSEM compared with the convection model of Eikerling et al. [5]. Membrane thickness 203 μm and $\lambda = 12.5$.

program and that $c^*_{H_2}$ could therefore be lumped into the constant ξ_2 in Eq. (8). In fact, over the hydrogen partial pressure and temperature ranges studied, $c^*_{H_2}$ varies by about a factor of two.

3.1.2. Ballard Power Systems Mark V PEMFC

Results from the Mark V cell, an approximately 1990 technology, have been published from this laboratory [19], although the published coefficient values contained several errors. A 35-cell stack was used in that study with each cell having an active cross-sectional area of 232 cm^2. Again, this stack had experienced intermittent operation over several years before the experimental measurements for the model development were carried out.

Referring to Eq. (8), corrected experimental values for the various coefficients are:

$$\xi_1 = -0.944 \quad \xi_2 = 0.00354$$

$$\xi_3 = 7.80 \times 10^{-5} \quad \xi_4 = -0.000196$$

Utilising these coefficients in the various terms of Eq. (8) gives:

(i) $\alpha_c = 0.56$ from ξ_4
(ii) $\alpha_c = 0.525$ from ξ_3
(iii) $\Delta G_{ec} + 3.68(\Delta G_e) = 1.822 \times 10^5$ J/mol
(iv) $k^0_c(c^*_{H^+})^{(1-\alpha_c)}(c^*_{H_2O})^{\alpha_c}(k^0_c)^{0.273} \cong 54.4$ to 60.7

Again the α_c values are above the range suggested by Berger [23] but are in good agreement with the values from the Mark IV study.

3.1.3. Coefficient values chosen for the GSSEM

From the above sets of coefficients from work in this laboratory on Mark IV and Mark V Ballard hardware, the following coefficient values are proposed for the GSSEM:

$$\xi_1 = -0.948(\pm 0.004)$$

$$\xi_2 = 0.00286 + 0.0002 \ln A + (4.3 \times 10^{-5}) \ln c^*_{H_2}$$

$$\xi_3 = (7.6 \pm 0.2) \times 10^{-5} \quad \xi_4 = -(1.93 \pm 0.05) \times 10^{-4}$$

Note that ξ_1 was obtained by a simple average of two published values. Also note that ξ_2, which previously included the cell active area, A, and the assumed-to-be-constant, $c^*_{H_2}$, now has both of these parameters appearing as items to be input or calculated.

4. Results: comparison of GSSEM predictions to experimental data

4.1. Ballard hardware and H_2 / air feed

The predictions of the GSSEM model were compared to data for the performance of both Mk. IV and Mk. V hardware. It should be noted that the GSSEM is configured so that other concentrations of oxygen in nitrogen, different than standard air, can be modelled. This could have applicability for situations where oxygen enrichment is used to improve cathode performance or where nitrogen dilution is used to control fuel cell voltage.

Fig. 1 is a parity plot, that is, the predicted performance of the cell based on the model versus the experimentally measured performance. The accuracy of the model is judged by the proximity of the data to a 45° line passing through the origin. Higher voltage data represent measurements at low current density, while low voltage data are for measurements at higher current density. As can be seen in Fig. 1, the model was able to predict accurately the performance of the Mark IV and V Ballard fuel cell hardware over a fairly large range of voltages representing current densities as high as 1.0 A/cm^2.

4.2. Ballard hardware and H_2 / O_2 feed

Performance curves illustrating the comparison between the predictions of the GSSEM and published experimental data for H_2/O_2 experiments are shown in Fig. 2. The value of λ for these data was set at 23.0 to represent a newer membrane. Such lack of fit that may be observed is mostly attributable to the divergence in the activation region of the polarisation curve.

4.3. Non-Ballard hardware

As indicated earlier, the numerical values of the empirical parameters of the GSSEM have been estimated from data obtained in this laboratory for Ballard hardware of about 1990 vintage. The validity of the GSSEM has been illustrated using this data and published data from Ballard in that same time period. The applicability of the GSSEM to represent the performance of other PEM fuel cells is illustrated in Figs. 3 and 4.

In Fig. 3 the GSSEM prediction is compared to data from Kim et al. [11] for a fuel cell using a Nafion 115 membrane. The GSSEM appears to reasonably represent the effect of reducing the membrane thickness.

Fig. 4 confirms that, for Nafion 117, the membrane that was used to develop the original values of the parameters, the GSSEM provides a reasonably accurate prediction of performance. Conversely, Fig. 4 shows that the model did not predict as significant an effect with temperature as was experimentally observed.

4.4. GSSEM prediction of membrane resistivity

As mentioned earlier, Eikerling et al. [5] have proposed a mechanistic model of membrane resistivity. Their model, however, is much more complex and computationally intensive than the GSSEM. In their work they present a comparison of their prediction for membrane resistance with the experimental measurements of Buchi and Scherer

[33]. Their model accurately predicted the membrane resistivity in the current density range of 0 to about 0.9 A/cm^2.

In Fig. 5 the prediction of the GSSEM is compared to the prediction of the convection model in Fig. 10 of Eikerling et al. [5]. As can be seen, the simpler approach of the GSSEM, which still retains a mechanistic basis, is also able to accurately predict membrane resistance.

5. Summary and conclusions

The proposed generalised steady-state electrochemical model (GSSEM) is broader in applicability than the earlier SSEM [18–22]. It now contains the capability of dealing, in a somewhat idealised way, with PEM fuel cells of any active area and Nafion membrane thickness up to relatively high current densities. Average membrane water content is considered, in a simplified way, via a single semiempirical parameter, λ.

It is clear from a review of published Nafion resistivity data that there is considerable variation arising from, for example, the method of membrane preparation/preconditioning type of flow field and the method of making experimental measurements, in situ or ex situ. This, coupled with the apparent variation in Nafion 117 thickness reported (175–222 μm), indicates that accurate prediction of the performance of every PEM cell utilizing Nafion is beyond the reach of a simple-to-use model.

The usefulness of the GSSEM lies in its largely mechanistic basis, giving it a flexibility in application to a wide range of operating conditions. The empirical expression for membrane resistance, through the adjustment of single coefficient, λ, should suffice for modelling all cells using Nafion membranes.

The simplifications and weaknesses of the GSSEM are:
- the assumption of an isothermal stack,
- the assumption that the gas flow rate and the design of the gas flow fields are sufficient to guarantee removal of excess liquid water,
- the assumption that $c^*_{H^+}$ and $c^*_{H_2O}$, in Eq. (6), are relatively constant and can be treated as constants in the evaluation of parameter ξ_2 in Eq. (8b).

In conclusion, the GSSEM is an extremely useful tool for simulation and design analysis of fuel cell power systems that allows the addition of parameters for fuel cell geometry and membrane characteristics in the design process.

6. Nomenclature

A	cell active area (cm^2)
$c^*_{H^+}$	proton concentration at the cathode membrane/gas interface (mol/cm^3)
$c^*_{H_2}$	liquid phase concentration of hydrogen at anode/gas interface (mol/cm^3)
$c^*_{H_2O}$	water concentration at the cathode membrane/gas interface (mol/cm^3)
$c^*_{O_2}$	oxygen concentration at the cathode membrane/gas interface (mol/cm^3)
E_{Nernst}	thermodynamic potential (V)
$\mathscr{F}$	Faraday's constant (96487 C/equ)
i	current (A)
k^0_a, k^0_c	intrinsic rate constants for the anode and cathode reactions, respectively (cm/s)
k'_c	modified rate constant cathode reactions (cm/s)
l	thickness of membrane layer (cm)
$p^*_{H_2}$, $p^*_{O_2}$	partial pressures of hydrogen and oxygen at the anode catalyst/gas interface and cathode catalyst/gas interface, respectively (atm)
r_M	membrane specific resistivity for the flow of hydrated protons (ohm cm)
T	cell temperature (isothermal assumption K)
ΔG_e	standard state free energy of chemisorption (J/mol)
ΔG_{ec}	standard state free energy of chemisorption (J/mol)

Greek

α_c	chemical activity parameter for the cathode.
$\eta_{act,a}$, $\eta_{act,c}$	the anodic and cathodic contributions to the cell activation overvoltage (V)
η_{ohmic}	ohmic contribution to cell overvoltage (V)
ξ_1, ξ_2, ξ_3, ξ_4	empirical coefficients for calculation of activation overvoltage
λ	semiempirical parameter representing the effective water content of the membrane, H_2O/SO_3^-

Acknowledgements

This work was funded by the Canadian Department of National Defence through a grant provided by the Chief of Research and Development.

References

[1] R.P. Iczkowski, M.B. Cutlip, J. Electrochem. Soc. 127 (1980) 1433.
[2] S.J. Ridge, R.E. White, Y. Tsou, R.N. Beaver, G.A. Eisman, J. Electrochem. Soc. 136 (1989) 1902.
[3] M.W. Verbrugge, D.M. Bernardi, AIChE J. 37 (1991) 1151.
[4] T.E. Springer, T.A. Zawodzinski, S. Gottesfeld, J. Electrochem. Soc. 138 (1991) 2334.
[5] M. Eikerling, Yu.I. Kharkats, A.A. Kornyshev, Yu.M. Volfkovich, J. Electrochem. Soc. 145 (1998) 2684.
[6] T.V. Nguyen, R.E. White, J. Electrochem. Soc. 140 (1993) 2178.
[7] J.S. Yi, T.V. Nguyen, J. Electrochem. Soc. 145 (1998) 1149.
[8] H. Ide, T. Yoshida, H. Ueda, N. Horiuchi, in: Proceedings of 24th

Intersociety Energy Conversion Conference, IECEC, 1989, pp. 1517–1522.
[9] J.C. Amphlett, M. Farahani, R.F. Mann, B.A. Peppley, P.R. Roberge, in: Proceedings of 26th Intersociety Energy Conversion Conference, IECEC, 1991, pp. 624–630.
[10] A. Cisar, in: Proceedings of 26th Intersociety Energy Conversion Conference, IECEC, 1991, pp. 611–616.
[11] J. Kim, S. Lee, S. Srinivasan, C.E. Chamberlin, J. Electrochem. Soc. 142 (1995) 2670.
[12] J.H. Lee, T.R. Lalk, A.J. Appleby, J. Power Sources 70 (1998) 258.
[13] D. Bevers, M. Wöhr, K. Yasuda, K. Oguro, J. Appl. Electrochem. 27 (1997) 1254.
[14] J.T. Hinatsu, M. Mizuhata, H. Takenaka, J. Electrochem. Soc. 141 (1994) 1493.
[15] T.E. Springer, M.S. Wilson, S. Gottesfeld, J. Electrochem. Soc. 140 (1993) 3513.
[16] S. Gottesfeld, T.A. Zawodzinski, Adv. Electrochem. Sci. Eng. 5 (1997) 195.
[17] J.S. Yi, T.V. Nguyen, J. Electrochem. Soc. 146 (1999) 38.
[18] R.M. Baumert, Master's thesis, Queen's University, Kingston, ON, Canada, 1993.
[19] J.C. Amphlett, R.M. Baumert, R.F. Mann, B.A. Peppley, P.R. Roberge, A. Rodrigues, J. Power Sources 49 (1994) 349.
[20] J.C. Amphlett, R.M. Baumert, T.J. Harris, R.F. Mann, B.A. Peppley, P.R. Roberge, J. Electrochem. Soc. 142 (1995) 1.
[21] J.C. Amphlett, R.M. Baumert, T.J. Harris, R.F. Mann, B.A. Peppley, P.R. Roberge, J. Electrochem. Soc. 142 (1995) 9.
[22] J.C. Amphlett, R.F. Mann, B.A. Peppley, P.R. Roberge, A. Rodrigues, Proceedings of the 10th Annual Battery Conference, 1995.
[23] C. Berger, Handbook of Fuel Cell Technology, Prentice Hall, Englewood Cliffs, NJ, 1968.
[24] P.C. Rieke, N.E. Vanderborgh, J. Membr. Sci. 32 (1987) 313.
[25] T. Nguyen, J.C. Hedstrom, N.E. Vanderborgh, Proc. Electrochem. Soc. (1989), 89 (Proc. Symp. Fuel Cells) 39.
[26] N.E. Vanderborgh, J.R. Huff, J. Hedstrom, in: Proceedings of 24th Intersociety Energy Conversion Conference, IECEC, 1989, p. 1637.
[27] T.F. Fuller, J. Newman, J. Electrochem. Soc. 139 (1992) 1332.
[28] D.P. Wilkinson, H.H. Voss, K. Prater, J. Power Sources 49 (1994) 117.
[29] T.F. Fuller, J. Newman, J. Electrochem. Soc. 140 (1993) 1218.
[30] D.S. Watkins, K. Dircks, D. Epp, C. De La Franier, Fourth Annual Battery Conf., 1989.
[31] K. Prater, J. Power Sources 29 (1990) 239–250.
[32] V.A. Paganin, E.A. Ticianelli, E.R. Gonzalez, Proc. 188th Meeting of the Electrochemical Society, 1995, pp. 297–304.
[33] F.N. Buchi, G.G. Scherer, J. Electroanal. Chem. 404 (1996) 37.